Int. J. Heat Mass Transfer. Vol. 11, pp. 1155–1165. Pergamon Press 1968. Printed in Great Britain

THE EFFECT OF RADIAL TEMPERATURE GRADIENT ON THE FORMATION OF AXIAL VOID IN UO_2 FUEL ELEMENTS

JACEK JEDRUCH*

Department of Nuclear Engineering, Pennsylvania State University, University Park, Pennsylvania 16802, U.S.A.

(*Received* 7 *August* 1967 *and in revised form* 6 *November* 1967)

Abstract—The process of axial cavity formation in UO_2 rods of nuclear fuel was investigated by means of a nodal model of heat transfer incorporating a space dependent heat source and both temperature and irradiation dependent thermal conductivity. The radii of the cavity and of the reorganized crystal zone were reproduced through calculation by postulating a progressive recrystallization of the initially porous UO_2, commencing at 1700°C, and associated with differential sublimation and condensation of UO_2, within the microscopic pores under the action of a high temperature gradient. The calculational model was found sufficient to predict quantitatively the experimentally observed changes in UO_2 rods and leads to the conclusion that the axial cavity may form before the UO_2 melting temperature of 2876°C is reached at the center of the rod.

NOMENCLATURE

A, heat-transfer area [cm^2];
B, zone coupling coefficient;
c, $\mathbf{C}$, thermal conductivity element and matrix [$W\,°C^{-1}$];
E, energy release in fission [$3{\cdot}2 \times 10^{-17}$ J $fission^{-1}$];
f, step function for UO_2 density;
h_{gap}, h_w, thermal conductance of gas, water film [$W\,cm^{-2}\,°C^{-1}$];
i, space position index;
K, thermal conductivity parameter [$W\,°C^{-1}$];
k_{unir}, k_{irr}, k_{zr}, thermal conductivity of unirradiated and irradiated UO_2, and Zircaloy-2 [$W\,cm^{-1}\,°C^{-1}$];
q''', volumetric heat source rate [$W\,cm^{-3}$];
q, $\mathbf{Q}$, point and vector heat source rate [W];
r, radial distance from center of pellet [cm];
t, $\mathbf{T}$, point temperature, temperature vector [°C];
u, radial distance expressed in neutron relaxation lengths;
v, velocity of void migration [Å s^{-1}];
V, volume [cm^3];
W, thermal resistance [$cm\,°C\,W^{-1}$].

Greek symbols

ρ_0, density of UO_2 crystal [$g\,cm^{-3}$];
ϕ, neutron flux [neutrons $cm^{-2}\,s^{-1}$];
Σ_f, macroscopic neutron fission cross section [cm^{-1}];
κ, reciprocal relaxation distance for neutrons [cm^{-1}].

1. INTRODUCTION

THE USE of UO_2 as fuel in nuclear reactors has led to the discovery of the spontaneous formation of an axial cavity in the UO_2 pellets under irradiation in a high neutron flux. If it is borne in mind that UO_2 is a very hard, porcelain-like ceramic material of high melting point (2876°C), and can normally be drilled only with great difficulty, using a supersonic or a diamond-tipped drill, the spontaneous appearance of

* Present address: Advanced Reactors Division, Westinghouse Electric Corporation, Madison, Pa. 15663, U.S.A.

an axial pinhole running the length of the fuel rod presents an interesting problem from both the materials and the heat transfer point of view.

UO_2 pellets used in nuclear fuel elements, are usually manufactured by compressing and sintering UO_2 powder in a helium atmosphere. The resulting material consists of small UO_2 crystals separated by microscopic voids filled with He, and its density is typically 0·95 of that of a solid crystal. When this material is subjected to neutron irradiation, fissions take place in the uranium, and the material becomes a high intensity heat source. The heat-transfer properties of the material undergo slow changes due to high temperature gradients, release of fission gases and accumulation of solid fission products. The physical structure of the material is altered and, if the neutron flux is sufficiently high, the axial cavity appears.

The fracture of the irradiated fuel, see Fig. 1, shows the characteristic axial hole, surrounded by an inner annular zone of radially oriented crystalline structure, and an outer zone of seemingly unaltered oxide.

Some investigators [2, 3] attribute the formation of the void and the zone of reoriented structure to the partial melting of UO_2 on irradiation and solidification shrinkage on subsequent cooling. While plausible as an explanation of the appearance of the fracture of fuel rods which have achieved heat fluxes above 200 W/cm^2, the formation of central voids in rods of UO_2 operated at heat fluxes as low as 140–160 W/cm^2, when central melting does not occur, is not adequately explained by the models of heat transfer proposed.

A better mechanism for the central void formation is suggested by the work of Gruber [4] who has shown that the microscopic voids existing in a solid will slowly migrate towards regions of high temperature if a high thermal gradient is present and the material is susceptible to sublimation. Thus, if a microscopic void has opposite walls at considerably different temperatures sublimation from the hot wall, and solidification on the cold wall may occur.

UO_2 is subject to sublimation [5] at temperatures above 1700°C and Nichols [6] estimates the velocity of void migration in it to be $v \simeq 15$ Å/s at $t = 1730$°C and the temperature gradient of $dt/dr \simeq 10^3$ °C/cm. At 1530°C the velocity of void migration is only 0·3 Å/s. Nichols distinguishes between the short-time phenomena, such as recrystallization and the central void formation which occur within tens of days and are attributed to the migration of fabricated porosities, and the long-time phenomena, such as swelling, fission gas release, etc., which occur in irradiations of the order of one year.

Here the investigation of the void formation was formulated for the condition of the UO_2 pellets in which the short-time phenomena are completed and the long-time phenomena are not yet felt. This is the condition for which experimental data used here were obtained.

It will be shown below that a heat-transfer model with the heat source following the distribution of fissions in UO_2 and the thermal conductivity dependent on temperature, density and irradiation history of UO_2, will predict a temperature gradient in UO_2 which is compatible with geometrical and internal changes observed experimentally on irradiation.

The experimental data on rod dimensions, heat fluxes, and dimensions of axial cavities was taken from [7], which reports the condition after irradiation of UO_2 rods of 0·9042 cm in diameter and clad with 0·0687 cm thickness of Zircaloy-2, and cooled with water. Heat fluxes attained during irradiation and spatial distribution of fissions in the UO_2 rod were also given. The density of UO_2 was reported as 0·95 of that of a solid crystal. The ratio of cold assembled diametral clearance between the clad and the pellet to the pellet diameter was 0·022.

The physical properties of UO_2 were taken in accordance with data in [5].

2. OUTLINE OF THE METHOD OF ANALYSIS

The analysis was based on recreation through a mathematical model of a static condition of the fuel at the end of the process of the void migra-

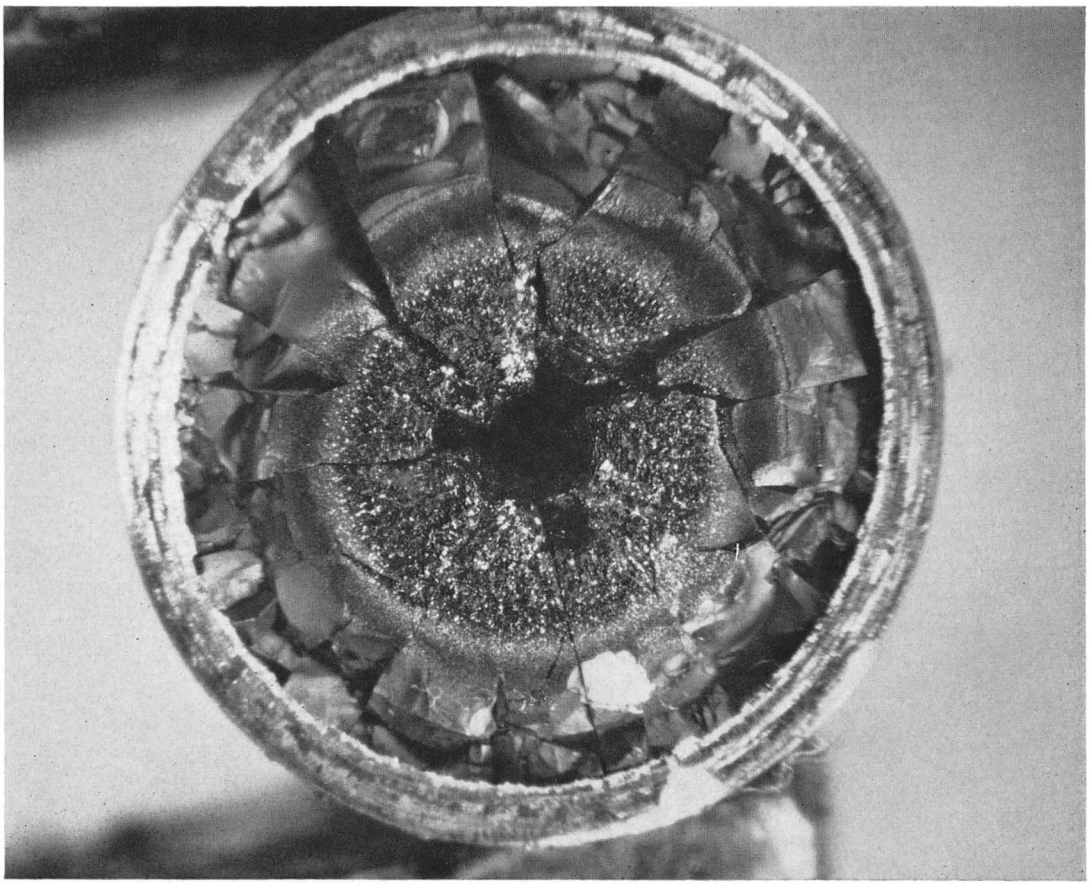

FIG. 1. Fracture of an irradiated UO_2 rod showing the center cavity, recrystallized zone, unaltered zone and metal clad tube.

tion through UO_2, i.e. the time dependence of the process was not considered.

A measured space distribution of fissions in UO_2 rods was converted to a functional relationship which was then used to calculate the space-dependent heat generation rate. Since fuel sectioning and the measurements of the diameter of the axial cavity are possible only in the cold condition, all dimensions were referred to that state.

The relationships predicting the change of UO_2 density with temperature, as well as the measured temperature dependence of UO_2 thermal conductivity, was used in an iterative procedure for solving simultaneously for the radial temperature distribution and the size of the axial cavity as a function of total heat output of the fuel elements. The calculations were performed by means of a nodal method and implemented for a digital computer.

Because of the high length to diameter ratio, common for nuclear fuel rods (usually greater than 100:1), the heat transfer in the axial direction forms an insignificant part of the whole and can be neglected. Thus only radial heat transfer need be considered.

3. DESCRIPTION OF PROBLEM GEOMETRY

The mathematical model was applied through a nodal analysis. The space nodes were located as indicated in Fig. 2. The radius of center void, r_N, is temperature dependent (see next section) and its magnitude is one of the principal results of this investigation.

The fuel section, $r_3 - r_N$, was divided into $N - 3$ equal increments, and the remaining nodal points were located at the inside and outside faces of the radial gas gap, on the outside of the clad, and in the coolant stream. The radial gas gap was assumed of uniform thickness along the circumference. At operating temperature, the two surfaces come into contact due to differential expansion.

4. VOLUME CHANGE OF UO_2 ON RECRYSTALLIZATION

All dimensions were referred to the cold

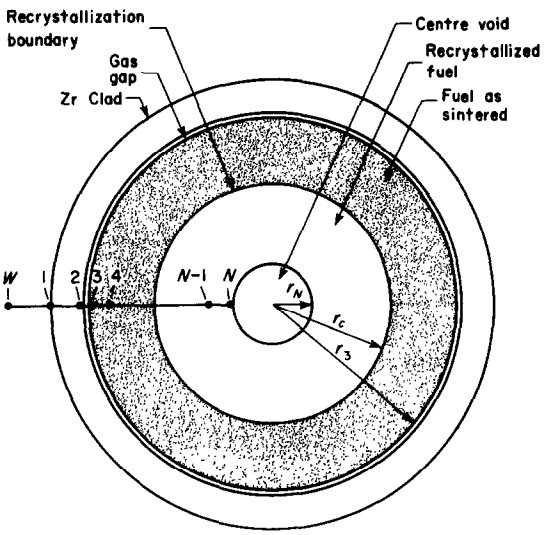

FIG. 2. Geometry used in calculation.

condition, i.e. they refer to dimensions at the time the fuel was sectioned and analyzed.

The density of UO_2 was assumed to be a step function of temperature once attained by the fuel, i.e.

$$\rho(t) = \rho_0 f \tag{1}$$

where

$$\rho_0 = 10{\cdot}96\ \text{g/cm}^3, \quad \text{density of } UO_2 \text{ crystal}$$
$$f = 0{\cdot}95, \quad 20^\circ\text{C} \leqslant t \leqslant 1700^\circ\text{C}$$
$$f = 1{\cdot}0 \quad t \geqslant 1700^\circ\text{C}.$$

Assuming that recrystallization boundary for a given constant heat flux is located at radius, r_c, the following equation can be written, see Fig. 2,

$$\pi[r_3^2 \rho_0 f] = \pi[(r_3^2 - r_c^2)\rho_0 f + (r_c^2 - r_N^2)\rho_0] \tag{2}$$

from which the relation between the void radius, r_N, and the recrystallization radius, r_c, was obtained

$$r_N = r_c \sqrt{(1 - f)}. \tag{3}$$

Thus the problem reduces to that of determining the position of the recrystallization boundary, r_c, i.e. the point at which the UO_2 temperature

reaches 1700°C. The maximum fractional void volume attainable at low burnup of the fuel equals, of course, $1 - f$.

5. DISTRIBUTION OF FISSIONS IN FUEL RODS

To calculate the space dependent steady-state temperature distribution in a fuel rod, the distribution of fissions in it is needed. The two quantities are connected through the equation

$$q'''(r) = E\Sigma_f\phi(r) \tag{4}$$

where:

- $q'''(r)$, volumetric heat generation rate [W/cm^3];
- $\Phi(r)$, neutron flux [neutron/cm^2/s];
- Σ_f, macroscopic fission cross section [fissions/neutron/cm];
- E, energy released in fission, $3{\cdot}2 \times 10^{-17}$ joule/fission.

The variation of the neutron flux with position in the UO_2 rod [8] can be obtained with accuracy sufficient for the purpose of this study from the solution of one-group neutron diffusion equation

$$\nabla^2\phi(r) - \kappa^2\phi(r) = 0 \tag{5}$$

where κ is the reciprocal relaxation distance for neutrons in UO_2. With only radial dependence considered, this equation becomes:

$$\frac{d^2\phi(r)}{dr^2} + \frac{1}{r}\frac{d\phi(r)}{dr} - \kappa^2\phi(r) = 0. \tag{6}$$

Substituting $u = \kappa r$, one obtains

$$u^2\frac{d^2\phi(u)}{du^2} + u\frac{d\phi(u)}{du} - u^2\phi(u) = 0 \tag{7}$$

which is a modified Bessel equation of order zero with the solution:

$$\phi(r) = AI_0(\kappa r) + BK_0(\kappa r). \tag{8}$$

Here I_0 and K_0 are modified Bessel functions of order zero of first and second kind, and A, B are constants.

The function K_0 goes to infinity at the origin, but on physical grounds the neutron flux is finite everywhere. Thus, in solid UO_2 rods only the I_0 solution is allowed in the form

$$q'''(r) = AE\Sigma_f I_0(\kappa r) = q_N'''I_0(\kappa r). \tag{9}$$

For rods with center cavity, the heat generating region no longer encloses the origin and in principle, the complete solution (8) applies. However, when investigating the inception of the void formation in the close vicinity of the origin the singularity of K_0 leads to gross disparity between the observed fission distribution and that predicted by equation (8). For this reason the heat source of the form of equation (9) will be used in the subsequent analysis.

The correct value of the constant κ, the neutron relaxation distance in the rod, is dependent on the enrichment of U in U-235 and is difficult to calculate accurately from first principles. It was obtained here directly from the distribution of fissions measured experimentally for the UO_2 rods which supplied the cavitation data.

The method used to obtain the value of κ was as follows. Experimental data on fission distribution in solid rods, as given in Table 1, were plotted on a semi-I_0 coordinate grid, i.e. the radius was marked off on a linear abscissa, and the corresponding fission rate on the I_0 ordinate, see Fig. 3. On such a plot data following the I_0 distribution will fall on a straight line and its slope will give the value of the reciprocal relaxation distance, κ. Here the data seems to

Table 1. Radial distribution of fissions in a fuel pellet

Radius (cm)	$\frac{\phi(r)}{\phi(0)}$	Radius (cm)	$\frac{\phi(r)}{\phi(0)}$
0·00	1·000	0·33	1·115
0·09	1·010	0·33	1·165
0·10	1·010	0·33	1·166
		0·33	1·181
0·17	1·025	0·33	1·213
		0·33	1·248
0·25	1·095		
0·25	1·092	0·470	1·309
		0·470	1·313
0·30	1·145		

UO_2 pellet, 94 per cent dense, 7·69 weight % U-235. Abstracted from [7], p. 157.

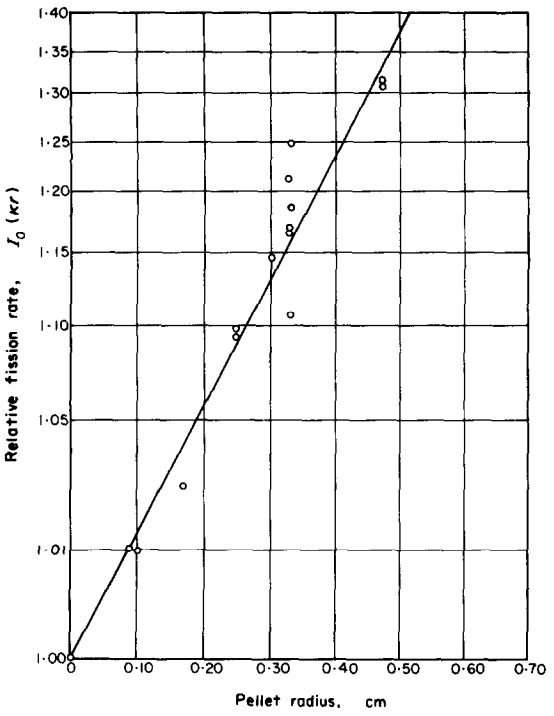

FIG. 3. Radial distribution of fissions in a UO_2 fuel rod.

follow the I_0 relationship well and gives $\kappa = 2{\cdot}38\ \text{cm}^{-1}$, the value used subsequently in calculating the volumetric heat source in rods which have not undergone recrystallization.

The radial fission distribution shown in Fig. 3 was measured for solid rods, i.e. without the central voids. It is expected that the operation with an axial cavity will introduce only small, second order perturbations to the I_0 distribution and the I_0 distribution will remain substantially unchanged, as long as the value of κ is appropriately modified.

The magnitude of the constant κ is directly proportional to the density of UO_2, and on its recrystallization increases to κ/f, where f is the initial fractional UO_2 density, as defined earlier. With a rod divided into two density zones, the neutron flux may be assumed to a first order approximation to have the form

$$\phi_1(r) = A_1 I_0(\kappa_1 r), \qquad r_N \leqslant r \leqslant r_c \quad (10)$$

$$\phi_2(r) = A_2 I_0(\kappa_2 r), \qquad r_c < r \leqslant r_3 \quad (11)$$

subject to the continuity boundary condition

$$\phi_1(r_c) = \phi_2(r_c) \quad (12)$$

where

$$\kappa_1 = \frac{\kappa_2}{f}.$$

Thus, in rods with center cavity and two density zones the heat source can be approximated by the forms

$$q_1'''(r) = q_N''' I_0(\kappa_1 r), \qquad r_N \leqslant r \leqslant r_c \quad (13)$$

$$q_2'''(r) = q_N''' \frac{I_0(\kappa_1 r_c)}{I_0(\kappa_2 r_c)} I_0(\kappa_2 r), \qquad r_c < r \leqslant r_3. \quad (14)$$

The notation used here for radii is the same as that in Fig. 2, and subscript 2 refers to fuel at the "as sintered" density.

6. VOLUMETRIC HEAT GENERATION RATE

Given the space dependence of heat generation of the form of equations (13, 14) and the experimental values of heat flux, q/A, through the outside fuel surface, the volumetric heat generation rate per unit length was normalized as follows:

$$\frac{q}{A} = \frac{2\pi q_N'''\left[\int_{r_N}^{r_c} r I_0(\kappa_1 r)\,dr + B\int_{r_c}^{r_3} r I_0(\kappa_2 r)\,dr\right]}{2\pi r_3}$$

$$= \frac{q_N'''}{r_3}\left[\frac{r_c I_1(\kappa_1 r_c) - r_N I_1(\kappa_1 r_N)}{\kappa_1} + B\frac{r_3 I_1(\kappa_2 r_3) - r_c I_1(\kappa_2 r_c)}{\kappa_2}\right] \quad (15)$$

where

$$B = \frac{I_0(\kappa_1 r_c)}{I_0(\kappa_2 r_c)},$$

so that

$$q_N''' = \frac{(q/A)\, r_3}{\dfrac{r_c I_1(\kappa_1 r_c) - r_N I_1(\kappa_1 r_N)}{\kappa_1} + B\dfrac{r_3 I_1(\kappa_2 r_3) - r_c I_1(\kappa_2 r_c)}{\kappa_2}}. \quad (16)$$

The subscript N denotes the innermost annulus and may equal, say twenty. If the rod is operated at such low q/A that the recrystallization does not take place and the axial cavity does not form, $r_N = 0$, $r_c = 0$ and the normalization becomes

$$q'''_N = \frac{(q/A)\,\kappa_2}{I_1(\kappa_2 r_3)}. \tag{17}$$

With the assumption of constant spacing between nodal points, Δr, the following holds for the heat source in the innermost annulus:

$$q_N = q'''_N\, 2\pi \int_{r_N}^{r_N + \frac{\Delta r}{2}} r I_0(\kappa_1 r)\,\mathrm{d}r$$
$$= \frac{q'''_N\, 2\pi}{\kappa_1}\left\{\left(r_N + \frac{\Delta r}{2}\right) I_1\left[\kappa_1\left(r_N + \frac{\Delta r}{2}\right)\right] - r_N I_1[\kappa_1 r_N]\right\}. \tag{18}$$

Similarly, for intermediate regions, up to r_c

$$q_i = \frac{q'''_N\, 2\pi}{\kappa_1}\left\{\left(r_i - \frac{\Delta r}{2}\right) I_1\left[\kappa_1\left(r_i - \frac{\Delta r}{2}\right)\right] - \left(r_i + \frac{\Delta r}{2}\right) I_1\left[\kappa_1\left(r_i + \frac{\Delta r}{2}\right)\right]\right\}. \tag{19}$$

From r_c to r_4 the heat source is

$$q_i = \frac{q'''_N\, 2\pi B}{\kappa_2}\left\{\left(r_i - \frac{\Delta r}{2}\right) I_1\left[\kappa_2\left(r_i - \frac{\Delta r}{2}\right)\right] - \left(r_i - \frac{\Delta r}{2}\right) I_1\left[\kappa_2\left(r_i + \frac{\Delta r}{2}\right)\right]\right\} \tag{20}$$

and for the outermost region, facing the gas gap:

$$q_3 = \frac{q'''_N\, 2\pi B}{\kappa_2}\left\{r_3 I_1[\kappa_2 r_3] - \left(r_3 - \frac{\Delta r}{2}\right) I_1\left[\kappa_2\left(r_3 - \frac{\Delta r}{2}\right)\right]\right\}. \tag{21}$$

For numerical calculations, the Bessel functions of second kind, zeroth and first order, I_0, I_1, were generated from the series:

$$I_0(x) = 1 + \frac{1}{(1!)^2}\left(\frac{x}{2}\right)^2 + \frac{1}{(2!)^2}\left(\frac{x}{2}\right)^4 + \frac{1}{(3!)^2}\left(\frac{x}{2}\right)^6 + \ldots \tag{22}$$

$$I_1(x) = \left(\frac{x}{2}\right) + \frac{1}{1!2!}\left(\frac{x}{2}\right)^3 + \frac{1}{2!3!}\left(\frac{x}{2}\right)^5 + \frac{1}{3!4!}\left(\frac{x}{2}\right)^7 + \ldots. \tag{23}$$

7. EQUATIONS FOR HEAT-TRANSFER COEFFICIENTS

The temperature dependence of the thermal conductivity of the unirradiated fuel is given by Scott [9] through the following relationship:

$$k_{\text{unir},\,i} = \frac{42{\cdot}0 f}{t_i + 400} \tag{24}$$

where:

t, temperature, at point i, [C°];
f, fraction of theoretical density (see Section 4).

For the irradiated fuel, such as investigated here, the thermal conductivity is given by Cohen [10] as:

$$k_{\text{irr},\,i} = \frac{k_{\text{unir},\,i}}{1 + W_{\text{irr}} \cdot k_{\text{unir},\,i}} \tag{25}$$

where $W_{\text{irr}} = 3{\cdot}44$ cm °C/W is the thermal resistance due to irradiation. The resulting variation of thermal conductivity of UO_2 with temperature is shown in Fig. 4.

Denoting by h the film or the gas gap heat-

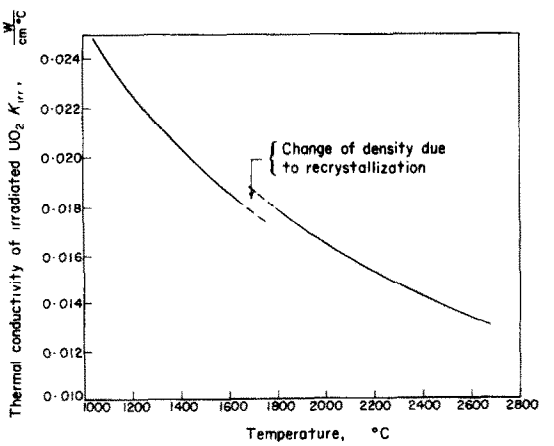

FIG. 4. Variation of thermal conductivity of irradiated UO_2 with temperature.

transfer coefficient we can write the following expressions for the constants in the heat balance

$$K_1 = h_w 2\pi r_1 \tag{26}$$

$$K_2 = k_{zr} \frac{2\pi\left[r_2 + \dfrac{r_1 - r_2}{2}\right]}{(r_1 - r_2)} \tag{27}$$

$$K_3 = h_{gap} 2\pi r_3 \tag{28}$$

$$K_i = k_{irr,i} \frac{2\pi\left[r_i + \dfrac{\Delta r}{2}\right]}{\Delta r}, i = 4, 5 \ldots, N \tag{29}$$

where

$$\Delta r = r_{i-1} - r_i = \frac{r_3 - r_N}{N - 3}. \tag{30}$$

The use of linear rather than logarithmic space averaging was possible here because of fine subdivision of space.

The values of the numerical constants used in the above equations are listed in Table 2.

The value of contact conductance of the clad-pellet interface was taken after Cohen [10] for the ratio of cold assembled diametral clearance to pellet diameter of 0·022 as here. The contact conductance replaces the gas gap at operating temperature due to differential expansion of UO_2 and Zircaloy-2 clad.

8. NODAL EQUATIONS OF HEAT BALANCE

When it is observed that the above equations for heat-transfer coefficients include the appropriate area elements of the form $2\pi[r_i + (\Delta r/2)]$, the following heat balance equations can be written on the assumption of zero azimuthal and axial heat flux; double subscripts identify interfaces between the nodes.

$$K_{2,1}(t_2 - t_1) + K_{w,1}(t_w - t_1) = 0$$

$$K_{1,2}(t_1 - t_2) + K_{3,2}(t_3 - t_2) = 0$$

$$K_{2,3}(t_2 - t_3) + K_{4,3}(t_4 - t_3) + q'''_3 V_3 = 0$$

$$K_{3,4}(t_3 - t_4) + K_{5,4}(t_5 - t_4) + q'''_4 V_4 = 0$$

$$\ldots$$

$$K_{N-2,N-1}(t_{N-2} - t_{N-1}) + K_{N,N-1}(t_N - t_{N-1}) + q'''_{N-1} V_{N-1} = 0$$

$$K_{N-1,N}(t_{N-1} - t_N) + q'''_N V_N = 0. \tag{31}$$

These equations can be written conveniently in the form of a tridiagonal matrix if we use the following notation:

$$q_i = q'''_i V_i$$

$$c_1 = K_{w,1}; c_2 = K_{2,1} = K_{1,2}, \text{ etc.}$$

$$\begin{bmatrix} (c_1 + c_2) & -c_2 & 0 & 0 & 0 & . & 0 \\ -c_2 & (c_2 + c_3) & -c_3 & 0 & 0 & . & 0 \\ 0 & -c_3 & (c_3 + c_4) & -c_4 & 0 & . & 0 \\ . & . & . & . & . & . & . \\ . & . & . & . & . & . & . \\ 0 & . & . & 0 & -c_{n-1} & (c_{n-1} + c_n) & -c_n \\ 0 & . & . & 0 & 0 & -c_n & c_n \end{bmatrix} \times \begin{bmatrix} t_1 \\ t_2 \\ t_3 \\ . \\ . \\ t_{n-1} \\ t_n \end{bmatrix} = \begin{bmatrix} c_1 t_w \\ 0 \\ q_3 \\ . \\ . \\ q_{n-1} \\ q_n \end{bmatrix}$$

or simply $\mathbf{CT} = \mathbf{Q}$

thus

$$\mathbf{T} = \mathbf{C}^{-1}\mathbf{Q}. \tag{32}$$

Since the elements of matrix $\mathbf{C}$ are temperature dependent through the temperature dependence of the thermal conductivity of UO_2, the solution of equation (32) requires an iterative approach. The calculation is always performed for a specified heat flux, q/A, for which the temperature distribution in UO_2, and the radii of the axial cavity and the recrystallization zone are required.

Table 2. Values of numerical constants used in this study

Quantity	Symbol	Value	Units	References
Neutron reciprocal relaxation distance	κ	2·38	cm^{-1}	Section 5
Contact conductance of clad–pellet interface	h_{gap}	0·35	$W/cm^2\,°C$	[10]
Thermal conductivity of Zircaloy-2	k_{zr}	0·167	$W/cm\,°C$	[11]
Water film heat-transfer coefficient	h_w	5·7	$W/cm^2\,°C$	[5]
Mean temperature of coolant water	t_w	332	°C	[7]
Recrystallization temperature of UO_2	t_c	1700	°C	[5]
Melting temperature of UO_2	t_m	2876	°C	[1]

The computational procedure used was as follows: a flat radial distribution of temperature in UO_2 and a solid rod ($r_N = 0$) were assumed initially. Heat source **Q** and the elements of matrix **C** corresponding to the solid geometry were calculated at this temperature. The inversion of matrix **C** and the calculation of the first iterate of the temperature vector $\mathbf{T}^{(1)}$ were done using standard mathematical methods. Once the first iterate of the temperature vector $\mathbf{T}^{(1)}$ was obtained, the elements of matrix **C** were recomputed for the corresponding temperatures and the second iterate of the temperature $\mathbf{T}^{(2)}$, obtained, and so on. This procedure is laborious, when performed by hand and thus the above equation is best solved with a digital computer.

When in the course of iteration for the solution of vector **T** for a specified value of q/A the temperature at the center of the rod was found to exceed 1700°C, the condition for void formation exists. The preliminary position of the recrystallization boundary was obtained from the space location of the element of the temperature vector where its magnitude exceeds 1700°C.

From the position of recrystallization boundary, r_c, the decrease of volume due to elimination of porosities in the region at temperatures above 1700°C was calculated, giving the first iterate of the radius of the cavity, r_N, from equation (3).

At this point the new radial positions of the nodal points in UO_2 were calculated, keeping their number constant and assuming equal spacing between them. The new elements of the heat source vector **Q** for the reduced volume were calculated from equations (18–21) and the elements of matrix **C** recalculated correspondingly.

Iterations involving recalculation of the thermal conductivity throughout the rod, the determination of the recrystallization boundary, and the radius of the void, were continued until the variation of the temperature of UO_2 at the surface of the cavity satisfied a specified convergence criterion, say, the successive iterations do not differ by more than 1 per cent for the maximum temperature attained in the fuel.

Generally four to five iterations were sufficient to generate a stable temperature on the surface of the inner cavity and to obtain its radius for a specified heat flux through the clad.

9. COMPARISON WITH EXPERIMENT AND DISCUSSION

In this study, the equation (32) was solved for the temperature vector **T** for a number of specified heat fluxes, q/A, through the outside surface of the fuel. The input values of q/A were chosen to cover the range for which experimental data on heat fluxes and void diameters were available in [7].

A typical temperature distribution calculated for a fuel rod with an axial cavity is shown in Fig. 5. A summary of results is given in Table 3 and Fig. 6 together with experimental results.

Examination of Fig. 6 reveals that the prediction of the position of the recrystallization

Table 3. Summary of experimental and calculated results

UO_2 of 95 per cent theoretical density, 7·8 per cent by weight of U-235 in U

Heat flux q/A (W/cm^2)	Axial void radius, r_N (cm) experimental*	calculated	Recrystallization zone radius, r_c (cm) experimental*	calculated	Calculated maximum temperature (°C)
142·6	0·057 ± 0·019	0·0590	0·273 ± 0·032	0·271	2223
147·3	0·127 ± 0·064	0·0606	0·260 ± 0·006	0·285	2321
149·2	0·127 ± 0·089	0·0595	0·292 ± 0·013	0·283	2326
153·6	0·079 ± 0·048	0·0640	0·248 ± 0·019	0·295	2412
160·3	0·073 ± 0·040	0·0696	0·279 ± 0·013	0·310	2533

* Experimental data taken from [7], Table 3.

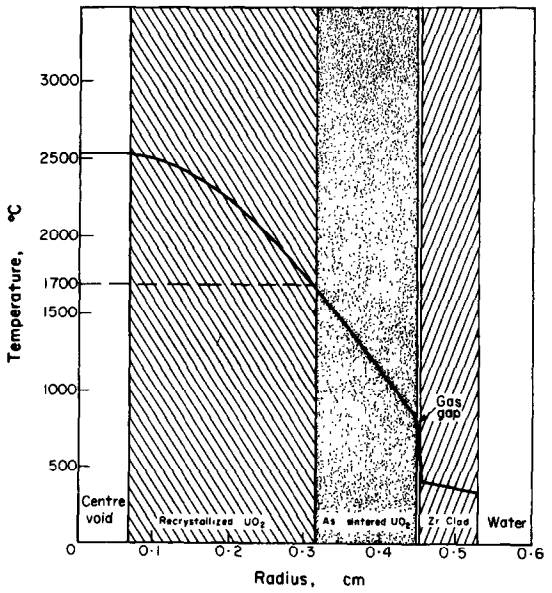

FIG. 5. Typical calculated temperature distribution in a UO_2 rod with axial cavity.

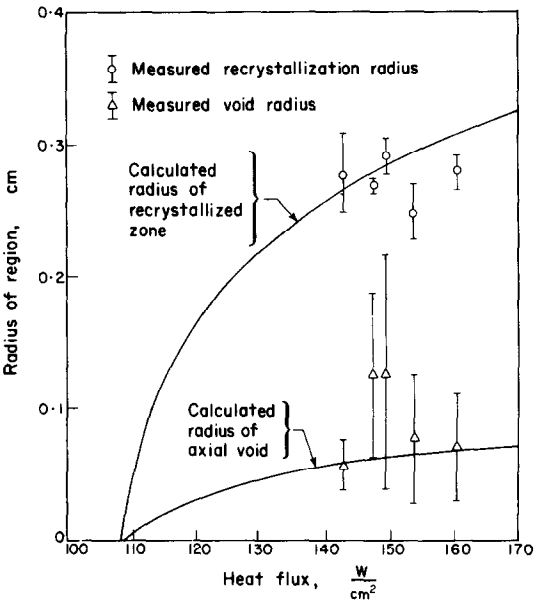

FIG. 6. Calculated and measured radii of voided and recrystallized regions.

boundary is considerably better than that of the center void. This can be understood from reference to Fig. 1, where the surface of the cavity is seen to be much more irregular, both absolutely and relatively, than that of the recrystallization boundary.

The method of analysis presented above and its results are compatible with the requirement for cavity formation that the temperature in the central region of fuel exceeds 1700°C, at which point the grain growth commences, and a somewhat porous sintered UO_2 (95 per cent of crystal density) recrystallizes and attains the density of a crystal. Contraction of the recrystallized central region results in cavity formation.

These results show that the mathematical model of heat transfer through the pellets presented here is capable of predicting the axial cavity formation in UO_2 fuel elements at temperatures well below the melting point of UO_2, i.e. below 2876°C, and thus constitutes a useful method for treating the phenomenon in the range of lower heat fluxes than that treated by other authors.

The results of calculations as presented in

Fig. 6 also indicate that no central void would be expected to form at power densities corresponding the surface heat fluxes of about 110 W cm^{-2}. In addition, the model presented here is simpler and more convenient to apply than that proposed by Nijsing [12] who gives a closed solution for the temperature distribution in fuel rods with variable heat source, but does not treat the case of central void formation in fuel rods on irradiation.

ACKNOWLEDGEMENTS

The author wishes to thank Professor Wallis A. Lloyd for encouragement and advice received in the course of preparation of this paper, and the personnel of the Computation Center of the Pennsylvania State University for their help in using the IBM-7074 computer.

REFERENCES

1. R. E. LATTAN and R. E. FRYXELL, Determination of the melting point of UO_{2+x}, *Trans. Am. Nucl. Soc.* **8**(2), 375 (1965).
2. T. J. KISIEL, Observations on the thermal performance of UO_2 rod specimens from post-irradiation examinations, Bettis Technical Review, WAPD-BT-6, Pittsburgh, Pennsylvania (January 1958).
3. D. R. DEHALAS and G. R. HORN, Evolution of uranium dioxide structure during irradiation of fuel rods, *J. Nucl. Mater.* **8**, 207–220 (1963).
4. E. E. GRUBER, On the theory of migration and coalescence of bubbles in solids, ANL-7079, Argonne National Laboratory, Argonne, Illinois (1965).
5. J. BELLE, editor, *Uranium Dioxide: Properties and Nuclear Applications*. U.S. Atomic Energy Commission, Washington, D.C. (1961).
6. F. A. NICHOLS, Behaviour of gaseous fission products in oxide fuel elements, WAPD-TM-570, Bettis Atomic Power Laboratory, Westinghouse Electric Company, Pittsburgh, Pennsylvania (1966).
7. J. D. EICHENBERG, P. W. FRANK, T. J. KISIEL, B. LUSTMAN and K. H. VOGEL, Effects of irradiation on bulk uranium dioxide, WAPD-183, Bettis Atomic Power Laboratory, Westinghouse Electric Company, Pittsburgh, Pa. (1957).
8. J. L. MEEM, *Two Group Reactor Theory*, p. 266, Gordon and Breach, New York (1964).
9. R. SCOTT, Thermal conductivity of UO_2, AERE-M/R-2526, Atomic Energy Research Establishment, Harwell, England (1958).
10. I. COHEN, B. LUSTMAN and J. D. EICHENBERG, Measurement of the thermal conductivity of metal-clad UO_2 rods during irradiation, WADP-228, Bettis Atomic Power Laboratory, Westinghouse Company, Pittsburgh, Pa. (1960).
11. H. ETHERINGTON, editor, *Reactor Handbook*. McGraw-Hill, New York (1958).
12. R. NIJSING, Temperature and heat flux distribution in nuclear fuel element rods, *Nucl. Engng Des.* **4**, 1–20 (1966).

Résumé—Le processus de la formation de cavités axiales dans des barreaux de combustible nucléaire de UO_2 a été étudié au moyen d'un modèle nodal de transport de chaleur combineé avec une source de chaleur dépendant de l'emplacement et d'une conductivité thermique dépendant à la fois de la température et de l'irradiation. Les rayons de la cavité et de la zone cristalline réorganisée ont été reproduites par le calcul en supposant une recristallisation progressive de l'UO_2 initialement poreux commençant à 1700°C, et associée avec une sublimation et une condensation différentielle de l'UO_2 à l'intérieur des pores microscopiques sous l'action d'un gradient de température élevé. Le modèle du calcul a été trouvé suffisant pour prédire quantitativement les changements observés expérimentalement dans les barreaux d'UO_2 et conduit à la conclusion que la cavité axiale peut seformer avant que l'on atteigne 2876°C, température de fusion de l'UO_2, au centre du barreau.

Zusammenfassung—Der Vorgang der Bildung axialer Hohlräume in UO_2-Stäben des Kernbrennstoffs wurde mit Hilfe eines diskreten Modells für den Wärmeübergang untersucht, wobei eine ortsabhängige Wärmequellendichte und eine von Temperatur und Bestrahlung abhängige Wärmeleitfähigkeit berücksichtigt wurde. Die Radien der Hohlräume und der umgewandelten Kristallzone wurden durch eine Berechnung wiedergegeben, die eine fortschreitende Rekristallisation des ursprünglich porösen UO_2, beginnend bei 1700°C, annimmt und von einer differentiellen Sublimation und Kondensation des UO_2 in den mikroskopischen Poren unter dem Einfluss eines hohen Temperaturgradienten begleitet wird.

Das Berechnungsmodell erwies sich als ausreichend für die quantitative Voraussage der experimentell beobachteten Veränderungen in einem UO_2-Stab und führt zu der Aussage, dass die axialen Hohlräume gebildet werden können ehe die Stabmitte die Schmelztemperatur von 2876°C erreicht.

Аннотация—Процесс образования осевой каверны в стержнях ядерного топлива исследовался с помощью узловой модели теплообмена, включающей источник тепла, зависящий от положения в пространстве, и теплопроводность, зависящую как от температуры, так и от облучения. Радиусы каверны и зоны рекристаллизации были рассчитаны постулированием прогрессивной рекристаллизации первоначально пористого UO_2 при начальной температуре 1700°C и связанного с различиями в сублимации и конденсации UO_2 внутри микроскопических пор под действием высокого градиента температуры. Расчетная модель может успешно использоваться для количественного расчета найденных экспериментально изменений в стержнях UO_2 и приводит к выводу, что осевая каверна может возникать до достижения в центре стержня температуры плавления 2876°C.